Upper Bound Analysis for Near-net Shape Forging of a Crown Gear Form

Seung-Dong Lee*, Won-Il Kim** and Yohng-Jo Kim**

* Department of Machine Design, Youngjin Junior College, Taegu 702-022, South Korea

** School of Mechanical and Automation Engineering, Kyungnam University, Masan, Kyungnam 631-701, South Korea

ABSTRACT

A kinematically admissible velocity field for near-net shape forging of a crown gear form is proposed. This takes into account the profiled shape of the teeth chosen by approximating these kinematically as radially straight taper teeth, (rectangular and trapezoidal teeth). The upper bound to the forging load, the relative forging pressure and the deformed configurations, with both the initially solid circular cylindrical and hollow billets, are predicted using the velocity field at varying incremental punch movements considering differing frictional factors. These and other results are given and commented upon.

Key Words : upper bound elemental technique, kinematically admissible velocity field, crown gear, near-net shape forging

Nomenclature

N, N_T : number of crown gear teeth

α, β : angle as shown in Fig. 3, ($\beta = \pi$ /N)

γ : pressure angle of gear tooth

h : current height of the block above the stationary die

h_t : height of the tooth, see Fig. 2

h_s : current height of the material at the corner filling stage as shown in Fig. 3

r_s : current radial distance at the corner filling stage as shown in Fig. 3

r_h, r_i, r_o : radial distances shown in Fig. 2(b)

ξ : angle ratio ($= \alpha / \beta$)

$\dot{u}_o$: velocity of the moving die(punch)

$\dot{W}_i$: internal plastic energy dissipation rate in each of the deformation zones

$\dot{W}_s$: energy dissipation rate due to velocity discontinuities on different surfaces

$\dot{W}_f$. frictional energy dissipation rates at die-material interfaces

$\dot{W}_T$: total energy dissipation rate

$\bar{\sigma}$, $\bar{\dot{\varepsilon}}$: effective stress, effective strain rate

$\dot{\sigma}_{ij}$: deviatoric stress component

r, θ, z : radial, hoop and axial distances (polar coordinate system)

$\dot{u}_r$, $\dot{u}_\theta$, $\dot{u}_z$: radial, hoop and axial velocity components

$\dot{\varepsilon}_r$, $\dot{\varepsilon}_\theta$, $\dot{\varepsilon}_z$: radial, hoop and axial strain rate components

$\dot{\gamma}_{r\theta}$, $\dot{\gamma}_{\theta z}$, $\dot{\gamma}_{zr}$: shear strain rate components (polar coordinate system)

$\dot{\varepsilon}_{ij}$: strain rate components

k : yield shear stress ($= \bar{\sigma}/\sqrt{3}$)

σ_o : flow stress

m : frictional factor $1 \geq m \geq 0$

F : punch/die load or power per unit downward velocity of the punch

1. Introduction

Crown gear is a component used in mechanical systems to transmit power and to convert velocity. Producing the gear of reduced weight but with increased strength results in saving energy and hence, there exists a strong demand for it. For this component, the closed-die forging process, which is moving more towards near-net shape forging, is a good manufacturing method that corresponds to this demand. The near-net shape forging can change an initial billet into a near-net shaped product which can be used directly as a part

requiring a little or no further finishing. The directional alignment of the grains or fibers, which forms the outline of the product during the forging process, helps improve mechanical properties of the final forged part with increasing strength, ductility, and resistance to impact and fatigue of the metal.

Usually overall performance of the forging operation requires not only an understanding of the flow stress of the material, the frictional conditions, but also the mode of flow of the material. Success here depends on a thorough understanding of the metal flow during forging. To acquire the knowledge necessary to design the forging processes, finite element method [1,2], upper-bound method [3-8] and upper-bound elemental technique [9-13] have been used to a great extent. Application of the upper bound elemental technique (UBET) to the forming analysis can be changed and adopted readily to the corresponding design parameters. Hence, the necessary information can be quickly retrieved to design the forming process. The UBET presented recently by Bramley[9] and Kiuchi[10] is a well-known theoretical method, and has been shown to be economical to analyse even some relatively complicated plastic forming problems. In order to use the UBET, the deforming body is first divided into several deformation zones or elements. The energy dissipation rates due to the plastic deformation in each of the divided zones or elements, at the element boundaries and that required to overcome frictional resistance at the die-metal interfaces are all then summed-up. Finally the design parameters which minimize the total energy dissipation are determined.

The upper bound approach was first presented by Kudo [4,5] in analysing axisymmetric and plane deformation problems. Upper bound analyses for closed-die forging of spur gear forms and splines [14-17] are found in the literature but little or no forging analysis of the crown gear form has been published though some work in gear coupling teeth [18] has appeared in the literature. In the present study, kinematically admissible velocity fields for the near-net shape forging analysis of a crown gear form are presented. In particular, the velocity fields corresponding to the tooth corner filling stage during forging of the crown gear form are also included. The upper bound simulation using the presented velocity field was done at incremental die movement stages for both the initial circular solid and hollow billets. The predicted values of the upper bound to the die loads and the deformed configurations of the tooth filling patterns based on CAD representations are compared with those observed experimentally in each case. The correlation between the experimental and the theoretical results was found to be reasonably good.

2. Forming processes and preform

The planning of the cold forging processes of a crown gear form is shown schematically in Fig. 1. It consists of five sub-processes; cutting of the billet, upsetting, extruding, piercing and closed-die forging. The first four of these processes make the preform to be forged during the final process of closed-die forging. Among these forging processes, the preform shape obtained after piercing for the hollow gear can strongly affect the forging result of the final forged product, especially the tooth corner filling of the final forging. To get a good quality forged product it is important to design the preform shape properly. For the proper design of the preform shape to produce a good quality product, the processing parameters should be investigated and then carefully controlled. Thus, the near-net shape forging process should in general be so designed that the proper preform for subsequent forging can also be obtained.

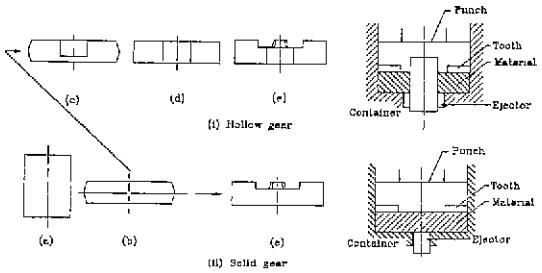

Fig. 1 Near-net shape forging processes of a crown gear form, (a) initial billet, (b) upsetting, (c) extrusion, (d) piercing, and (e) closed-die forging

3 Upper bound elemental analysis

3.1 Basic assumptions

In applying the upper bound elemental technique to the analysis of metal forming problems, several simplified assumptions are usually invoked. Those commonly used are;

i) the workpiece is homogeneous and isotropic,

ii) elastic deformations are neglected,

iii) the process is either frictionless or a constant shear

stress $\tau=mk$ where, $0\le m\le 1$ condition prevails at the tool-workpiece interface, here, k is the yield shear stress of the material,

iv) the inertia force of the deforming body is neglected,

v) the material flows according to the von Mises' flow rule, $k=\bar{\sigma}/\sqrt{3}$, where $\bar{\sigma}$ is the effective stress,

vi) the effect of strain hardening of the flow stress is not taken into account.

3.2 Kinematically admissible velocity fields

In obtaining power dissipation rates in a deforming body using an upper bound elemental technique, an admissible velocity field has to be postulated. It may also be advantageous to first divide the deforming body into several zones of deformations. In each of the individual zones, the velocity field and its derivatives should be continuous, and the normal component of velocity across the boundaries between two neighbouring regions should also be continuous. Some of these boundaries may be the velocity discontinuity planes. During the incremental forging of the crown gear form, in general, the plastic flow patterns and the velocity discontinuity boundaries in the deforming body will continue to change as the deformation progresses. However, in the present study, the velocity discontinuities were assumed, and for the convenience of simulation of the upper bound elemental analysis, not to change during the deformation.

Since, the crown gear form being analysed was symmetric about a diametral plane along the axial direction, the initial billet was therefore first divided into 2N similar segments, where N represented the number of teeth. Each of these divided segments was then again subdivided into 4 different deforming subzones, as shown in Fig. 3. Then for a downward axial velocity $\dot{u}_o$, of the moving punch with the gear teeth (rectangular or trapezoidal shapes), the velocity components for each of the divided subzones may be determined, using the equation of volume constancy and the boundary conditions of continuity. As the forging progresses, i.e. at the first stage, the billet material filling in the tooth cavity first gets in contact with the tooth root on the circumference of the punch head and then flows-in to fill into the inner tooth corner, where the second plastic flow stage is said to occur at the tooth corner filling stage. At this stage, for a comprehensive analysis of the formed tooth portion of the billet, it was again divided into three subzones for both the rectangular and trapezoidal shaped teeth respectively, as is shown in Fig. 3. Each of the corresponding velocity components is given in Table 1.

Table 1 Kinematically admissible velocity fields

Zone	Velocity components
Zone 1	$\dot{u}_r=0,\ \dot{u}_\theta=-\dot{u}_o\frac{r(\beta-\theta)}{h},\ \dot{u}_z=-\dot{u}_o\frac{z}{h}$, where $\beta=\pi/N$ (N=Number of teeth)
Zone 2	$\dot{u}_r=\dot{u}_o\frac{\beta r}{2ah}\left\{1-\left(\frac{r_h}{r}\right)^2\right\},\ \dot{u}_\theta=-\dot{u}_o\frac{ar\theta}{h},$ $\dot{u}_z=-\dot{u}_o\frac{z}{h}$, where $a=\frac{\beta}{\alpha}-1,\ a=\xi\beta\ (0<\xi<1)$
Zone 3	$\dot{u}_r=\dot{u}_o\frac{b(r_o-r)}{h},\ \dot{u}_\theta=-\dot{u}_o\frac{ar\theta}{h},$ $\dot{u}_z=\dot{u}_o c_r(r)\frac{z}{h}$, where $b=\frac{\beta r_t}{2a(r_o-r_t)}\left\{1-\left(\frac{r_h}{r_t}\right)^2\right\}$, $c_r(r)=a+b\left(2-\frac{r_o}{r}\right)$
Zone 4	$\dot{u}_r=0,\ \dot{u}_\theta=\frac{-\dot{u}_o c_r(r)\tan\gamma\ r_t\ r\ \theta}{a\ r_t\ r-\tan\gamma(r+r_t)(z-h)}$, $\dot{u}_z=\dot{u}_o c_r(r)\left\{1-\frac{r_t\tan\gamma(z-h)}{a\ r_t\ r-\tan\gamma(r+r_t)(z-h)}\right\}$
Zone 4-1	$\dot{u}_r=-\dot{u}_o\frac{r}{2h_t}\left[(1+a)\left\{\left(\frac{r_o}{r}\right)^2-1\right\}+2b\left(\frac{r_o}{r}-1\right)\right],\ \dot{u}_\theta=0$ $\dot{u}_z=\dot{u}_o\left\{(1+c_r(r))\left(\frac{h_m-z}{h_t}\right)-1\right\}$ where $h_m=h+h_t$
Zone 4-2	$\dot{u}_r=-\dot{u}_o\frac{c_{rs}(r-r_t)}{r_s-r_t},\ \dot{u}_\theta=-\dot{u}_o\frac{\tan\gamma}{a}c_r(r)\theta$ $\dot{u}_z=\dot{u}_o\left[c_r(r)+\left\{\frac{c_{rs}}{r_s-r_t}\left(2-\frac{r_t}{r}\right)+\frac{\tan\gamma c_r(r)}{ar}\right\}(z-h)\right]$, where $c_{rs}=\frac{r_t}{2h_t}\left[(1+a)\left\{\left(\frac{r_o}{r_s}\right)^2-1\right\}+2b\left(\frac{r_o}{r_s}-1\right)\right]$
Zone 4-3	$u_r=-\dot{u}_o\left[\frac{c_{rs}r_s}{r}+d\left(\frac{r_s}{r}-1\right)+\frac{er}{2(h_t-h_s)}\left\{\left(\frac{r_s}{r}\right)^2-1\right\}\right]$ $\dot{u}_\theta=-\frac{\dot{u}_o\tan\gamma r_o u_{hs}(r_t)\theta}{ar_o-h_s\tan\gamma},$ $\dot{u}_z=\dot{u}_o\left[u_{hs}(r)-e\left\{\frac{z-(h+h_s)}{h_t-h_s}\right\}\right]$, where $u_{hs}(r)=c_r(r)+\frac{c_{rs}h_s}{r_s-r_t}\left(2-\frac{r_t}{r}\right)$, $d=\frac{\tan\gamma r_o u_{hs}(r_t)}{ar_o-h_s\tan\gamma},\ e=1+u_{hs}(r_s)$

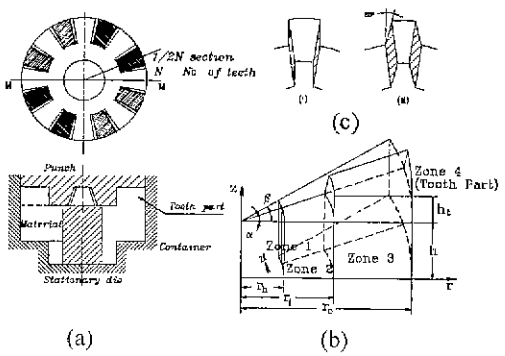

Fig 2 Subdivision of a deforming body into several subzones, (a) forging of a crown gear form with a hollow initial billet, (b) divided subzones and (c) shapes of the teeth, (i) shape of the rectangular teeth (γ=0°) and (ii) shape of the trapezoidal teeth, (γ=20°)

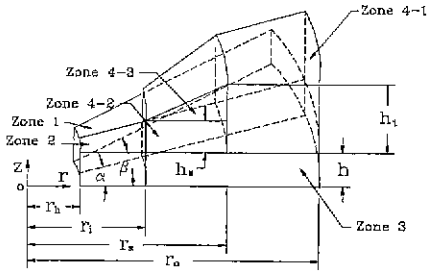

Fig. 3 Subzones of the tooth portion at the tooth corner filling stage.

3.3 Upper bound elemental solution

The strain rate components at any point in the deforming body in a cylindrical coordinate system are given by

$$\dot{\varepsilon}_r=\frac{\partial \dot{u}_r}{\partial r},\quad \dot{\varepsilon}_\theta=\frac{\dot{u}_r}{r}+\frac{1}{r}\frac{\partial \dot{u}_\theta}{\partial \theta},\quad \dot{\varepsilon}_z=\frac{\partial \dot{u}_z}{\partial z}$$

$$\gamma_{r\theta}=\frac{1}{2}\left[\frac{1}{r}\frac{\partial \dot{u}_r}{\partial \theta}+\frac{\partial \dot{u}_\theta}{\partial r}-\frac{\dot{u}_\theta}{r}\right]$$

$$\gamma_{\theta z}=\frac{1}{2}\left[\frac{\partial \dot{u}_\theta}{\partial z}+\frac{1}{r}\frac{\partial \dot{u}_z}{\partial \theta}\right],$$

$$\gamma_{zr}=\frac{1}{2}\left[\frac{\partial \dot{u}_z}{\partial r}+\frac{1}{r}\frac{\partial \dot{u}_r}{\partial z}\right]$$

where the dot(˙) represents the derivative of a variable with respect to time.

Here, the material in the analysis is considered rigid-plastic and is assumed to obey the von Mises yield criterion. The effective stress, $\bar{\sigma}$ and the effective strain rate $\bar{\dot{\varepsilon}}$ in the tensor form are, respectively, given by

$$\bar{\sigma}=\left[\frac{3}{2}\sigma'_{ij}\sigma'_{ij}\right]^{1/2} \tag{2}$$

and

$$\bar{\dot{\varepsilon}}=\left[\frac{2}{3}\dot{\varepsilon}_{ij}\dot{\varepsilon}_{ij}\right]^{1/2} \tag{3}$$

where $i, j=r, \theta, z$ and prime (') represents the deviator of the stress.

The upper bound solution suggested by Prager and Hodge[3] was that if there was no surface traction and the strain hardening effect was neglected, then

$$J=\sum\int_V \bar{\sigma}\bar{\dot{\varepsilon}}dV+\sum\frac{\sigma_o}{\sqrt{3}}\int_{S_v}|\Delta u|_{S_v}dS$$
$$+\sum\int_{S_t} m\frac{\sigma_o}{\sqrt{3}}|\Delta u|_{S_t}dS \geq \dot{W}_T \tag{4}$$

where $\sigma_o=\sqrt{3}k$ and k is the yield shear stress.

When the total deforming volume is divided as several sub-zones, the upper bound solution can be obtained by summing-up of all the individual energy dissipation rates for each of the subdivided zones. The total energy dissipation rates in closed-die forging, $\dot{W}_T$ is obtained by summing-up each of the internal energy dissipation rates due to plastic deformation over the volume, shear energy dissipation rates along the velocity discontinuity surfaces and the frictional energy dissipation rates along the tool-material interfaces, i.e.

$$\dot{W}_T=2N(\dot{W}_i+\dot{W}_s+\dot{W}_f) \tag{5}$$

where $\dot{W}_i=\int_V\bar{\sigma}\bar{\dot{\varepsilon}}dv$, $\dot{W}_s=\frac{\sigma_o}{\sqrt{3}}\int_{S_u}|\Delta \dot{u}_{S_u}|dS$,

$$\dot{W}_f=m\frac{\sigma_o}{\sqrt{3}}\int_{S_t}|\Delta \dot{u}_{S_t}|dS \tag{6}$$

where, m is friction factor, $0\leq m\leq 1$ and N represents the number of teeth. The strain hardening effect of the forged material was considered in calculating the upper bound solution. The applied force for a downward velocity, $\dot{u}_o$ of the punch for a closed-die forging is then determined as

$$F=\frac{\dot{W}_T}{\dot{u}_o} \tag{7}$$

4. Upper bound solution

An upper bound solution for the near-net shape forging of the crown gear form with either the rectangular or trapezoidal teeth can be obtained

numerically by using the velocity components presented previously. In obtaining the upper bound solution numerically, Simpson's rule was used for the various integral terms occurring on the work rate terms during the operation and the computer programme for their estimation was written using Fortran code.

To investigate the plastic flow patterns during the forging process, it is recommended that the distortion of grids marked on a typical cross section of the specimen should be checked. In other words, grids are first marked on the typical cross section of the deforming body before the forging process is conducted and then the nodal velocities are found for each of the forging processes. The coordinates of the grids are updated newly afresh at each incremental stage by using the nodal velocities and from these the material flow patterns can be obtained. Any position in the formed body during the forging process can be determined easily using the velocity components obtained for each of the divided subzones, that is, whenever the velocity components for each of infinitesimal deformation steps are obtained, the deformed geometry of the workpiece can also be obtained by updating the coordinates of the nodes in the following manner,

$$X^{i+1} = X^i + \dot{u}^i \Delta t \tag{8}$$

where X^i and X^{i+1} represent the coordinates of the grid nodes at the ith and the $(i+1)$th step of the deformation process, and Δt is the time-increment. $\dot{u}^i$ is the velocity component of a typical node at the ith deformation step. Therefore, in order to investigate the plastic flow pattern of the billet during the forging process, the nodal coordinates were updated for every infinitesimal time increments by using equation (8) and then the updated coordinates were displayed under the AutoCAD environment, this was done following yet another computer program developed by the author for the purpose The upper bound simulation was performed in the manner that the initial billet was deformed incrementally by giving 2% height reductions at each of the loading step.

5 Experimental works

Some approximation and simplifying assumptions are inevitable in almost all the theoretical analyses that are advanced to analyse metal forming processes, it is therefore, desirable to check their adequacy by performing experimental work in the laboratory under controlled conditions. Again certain important parameters that need to be used in the analysis can only be examined or verified by experiments. The general aim of the experimental work described here is determine the deformation forces, and the characteristic deformation modes that are met with during the process of metal flow in closed-die forging of the crown gear form, when material of the billet fills into the tooth cavity and also the tooth corner, in order to improve dimensional accuracy of the forged products.

5.1 Experimental materials

A few engineering materials such as, plasticine, wax, lead and aluminium have often been used as model materials for experimental investigation into the practice of metal forming. Among these, plasticine and tellurium(Te) lead are used extensively as model materials in experimental work since, at room temperature these represent almost similar physical properties and nearly the same flow pattern as that observed during working of steel at high temperature (about 1000°C). In the present work, Te-lead was chosen as the model materials for the experiments.

For most model materials, when experiments are carried out in the quasi-static state, the sensitivity of strain rate may be neglected, even though the effect of strain rate on the flow stress of the model material is reported[16]. Considering the effect of strain rate, the stress-strain relation for the model materials may be expressed by

$$\bar{\sigma} = C\,\bar{\varepsilon}^{n}\,\dot{\bar{\varepsilon}}^{m} \tag{9}$$

where C is a plasticity coefficient, n is the strain-hardening exponent and m the strain rate exponent. Here, the effect of strain rate will be neglected because the quasi-static forging process is only considered. Te-lead was selected as the model material for the experimental works. The flow stress is expressed by $\bar{\sigma} = 31.4\,\bar{\varepsilon}^{0.21}$(MPa) which was based on the results obtained from the compression test done on a cylindrical specimen.

5.2 The test specimens

To gain an insight into the flow of material during quasi-static closed-die forging of tellurium-lead specimens, a few sets of axially split-type half specimens were manufactured and produced from two solid specimens each. This was done by milling half of each

of these solid specimens to obtain exact halves. A square grid pattern of 1.5 mm × 1.5 mm was scribed on the meridional plane on one of these half split-type specimens that made a pair. To produce these grid lines, a vernier height gauge with a fine scribing edge was utilised. All the test specimens were manufactured as the circular solid billet of ϕ 38.0 mm × 10.2 mm. The shapes of specimens used for these experiments were chosen as the same dimension as that used for the upper bound simulation.

5.3 Experimental equipment

For the experimental investigations, a basic experimental apparatus was made. The forging apparatus consisted of a cylindrical container, a punch, a punch head and a die retaining ring. During the experimental investigations on quasi-static forging of the crown gear form, a computerized Instron 4400 series testing instrument (model 4485) of 200 kN capacity was used in conjunction with the sub-press assembly. All the experiments were carried out at the room temperature. The load-displacement curves and experimental data were obtained as a file using the computer control connected to the testing machine.

During the tests, the cross-head speed was set to 2.0 mm/min and was kept constant which prevented variation in mean effective stress in the specimen. The load was recorded at every 0.002 mm movement of the cross-head and was stored automatically in the data files. The load- displacement plot was also obtained from a plotter for each of these tests.

6. Presentation of results and discussions

6.1 Plastic flow pattern

The incremental upper bound simulation can yield tooth cavity filling patterns that may be produced following the computational procedure adopted of the near-net shape forging of an initially circular solid billet with parallel flats at its ends. Figures 4(a), 4(b) and 5(a), 5(b) show the resultant CAD outputs of the tooth forming patterns at different stages of the forging processes of the crown gear form each with 8 teeth under the friction condition of m=0.2 for both the initially circular solid and hollow billets. The results shown in Figs. 4(a) and 4(b) are for the rectangular teeth while, those shown in Figs. 5(a) and 5(b) are for the trapezoidal teeth. For comparison Figs. 6(a), 6(b), 7(a) and 7(b) show photographic views of the incremental deformed solid crown gear forms with the rectangular and trapezoidal teeth respectively. Again, Fig. 8 shows typical views of the profile geometry changes estimated at different increments in one of these forging process. From Fig. 4 to Fig. 8 it can be seen that the outer part of the workpiece top surface first gets in contact with the tooth root of the moving punch and then the inner corner of the tooth is filled completely. Regardless of the billet types, it may be seen that severe distortion of the grids marked on the cross sections takes place at the inner corner portion of each of the teeth. From these results, it may be expected that any failure such as folding or crack, if it may take place, would be at the inner tooth corner portion. Therefore, such a forging process for the final forging of the crown gear form may not be suitable for getting an excellent forged product. In practice, multi-forging processes and a proper preform shape is selected in order to obtain an excellent final product. Thus, there is a necessity for the design of a proper preform shape, which improve the dimensional accuracy of the final forged crown gear form. This should be selected in a manner that the billet material can fill in both the outer and the inner corners of the tooth root of the moving punch simultaneously.

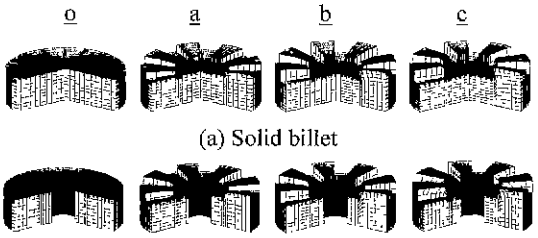

(a) Solid billet

(b) Hollow billet

Fig. 4 Tooth forming patterns during the forging process (rectangular teeth, upper bound simulation, N_T=8)

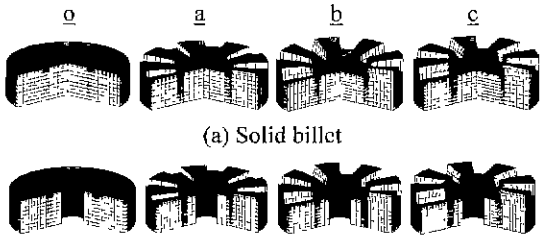

(a) Solid billet

(b) Hollow billet

Fig. 5 Tooth forming patterns during the forging process (trapezoidal teeth, upper bound simulation, N_T=8)

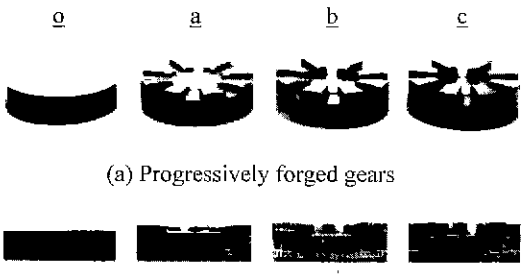

(a) Progressively forged gears

(b) Their sectioned views

Fig. 6 Photographic views of the incremental deformed form with solid billets of Te-lead (N_T=8, rectangular teeth, $\gamma = 0^\circ$, h_o/d_o=0.27, d_o=38mm, r_t=9mm, h_t=3.8mm)

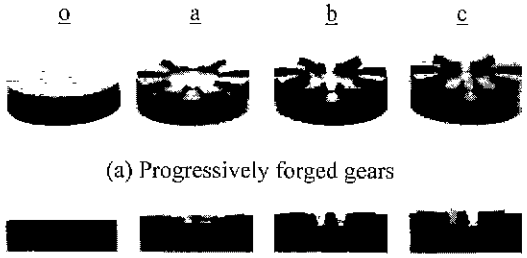

(a) Progressively forged gears

(b) Their sectioned views

Fig. 7 Photographic views of the incremental deformed form with solid billets of Te-lead (trapezoidal teeth, $\gamma = 20^\circ$, N_T=8, h_o/d_o=0.27, d_o=38mm, r_t=9mm, h_t=3.8mm)

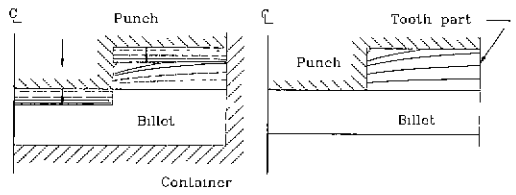

(a) (b)

Fig. 8 Profile geometry changes estimated by UBET during the forging process, (a) tooth filling flow according to the incremental punch movement and (b) change of the billet contour in the tooth part.

6.2 Die load-die movement curves and profile geometry changes

The experimental results of quasi-static closed-die forging of crown gear forms on Te-lead specimens were first observed in the form of autographic diagrams of the die load vs die movement curves. Typical Figs. 9(a) and 9(b) show the autographic diagrams of the die load vs die movement for closed-die forging of the crown gear forms from solid cylindrical specimens of Te-lead. Each of the crown gear forms consists of four and eight teeth, and rectangular and trapezoidal in shape. The initial diameter of the billet was 38.0 mm while the height was 10.2 mm. The whole tooth depth of the toothed punch was 3.8 mm. irrespective of the tooth shapes and the pressure angle for the trapezoidal tooth was 20°. The figures reveal that the estimated forging load on the crown gear with eight teeth is a little high than that of four teeth, as would be expected. Two flexion points on these curves are shown, where the first flexion point can be due to initiation of deformation flow at both inner and outer diameter sides of tooth, while the second flexion point is explained as the tooth corner filling stage. These figures show that the forging load increases rapidly at the corner filling stage

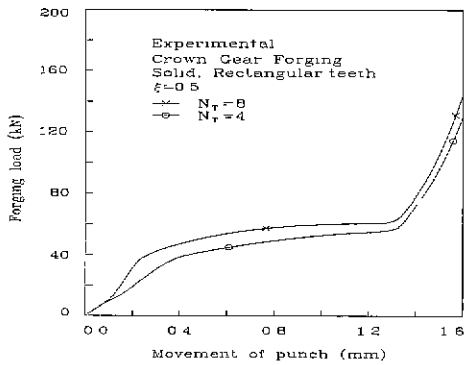

(a) Rectangular teeth

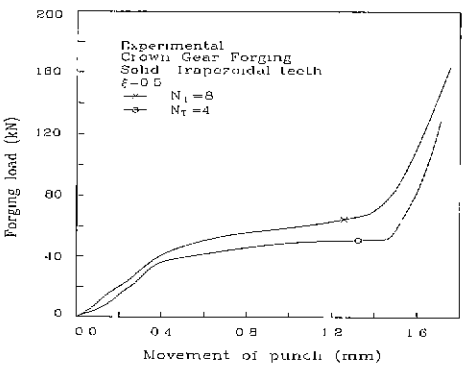

(b) Trapezoidal teeth

Fig. 9 Die load vs die movement for closed-die forging of a crown form from solid cylindrical specimens of Te-lead, (N_T=4 and 8, ξ=0.5)

Figures 10(a) and 10(b) show some repeated test results (die load-die movement curves) for the specimens forged incrementally to the die movement stages, where a, b and c marked on these curves indicate the current shapes of the deformed specimens corresponding to these stages. The photographic evidence showing the isometric and plan views of the progressively deformed specimens at these stages a, b, and c, are given in Figs. 6(a-b) and 7(a-b), respectively.

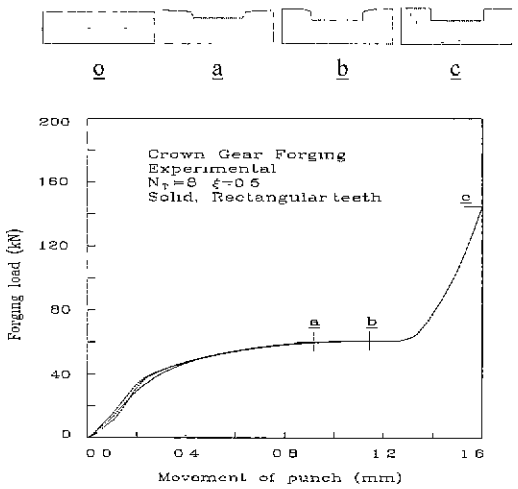

(a) Rectangular teeth (γ=0°)

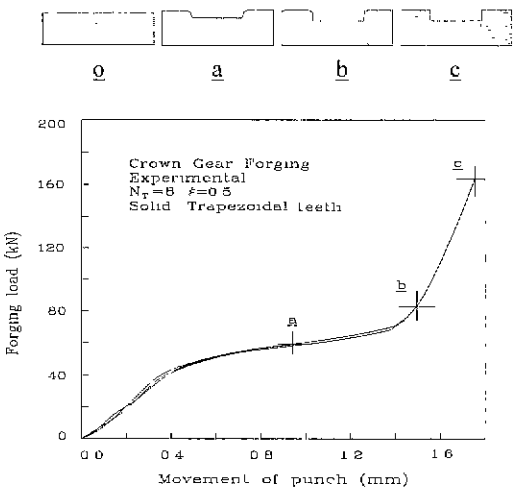

(b) Trapezoidal teeth (γ=20°)

Fig. 10 Profile geometry changes during the forging process of solid cylindrical specimens of Te-lead, (N_T=8, ξ=0.5, h_o/d_o=0.27, d_o=38mm, r_t=9mm)

6.3 Theoretically estimated relative pressure and forging load

To obtain the estimated results of forging loads and the relative pressure, based on the incremental upper bound simulation followed, the flow stress equation was selected by $\bar{\sigma}$= 31.4 $\bar{\varepsilon}$0.21(MPa), which was based on the results obtained from the compression test done on a cylindrical specimen made of Te-lead. Figs. 11(a) and 11(b) show the variation of the relative pressures for forging of the crown gear forms with the 4 and 8 teeth, each with the rectangular and trapezoidal shape teeth respectively, under the friction conditions of m=0.2 and 0.4 using the solid and hollow billets. The results given in Fig. 11(a) is for the rectangular teeth while Figs. 11(b) is for the trapezoidal teeth.

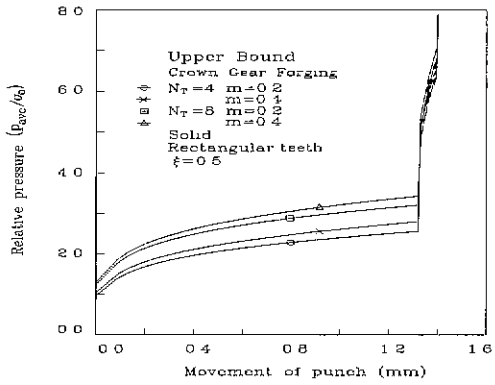

(a) Rectangular teeth

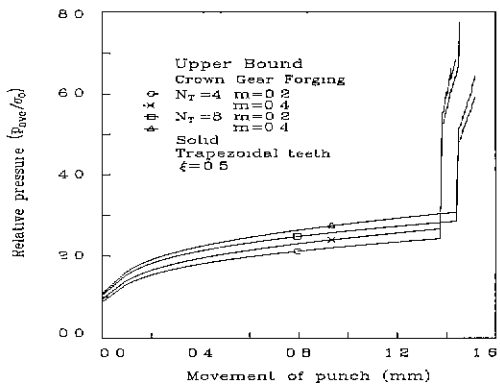

(b) Trapezoidal teeth

Fig. 11 Relative forging pressure according to punch movement (solid billet, N_T=4 and 8, theoretical)

It may be seen from these figures that the relative forging pressures for forging of the rectangular teeth, Fig. 11(a), is slightly greater than that for the trapezoidal teeth, Fig. 11(b). This is because the flow in tooth cavity filling during forging of the trapezoidal teeth is relatively much easier than that in forging of the rectangular teeth and also that the dimensions of the divided subzones are different in these two cases. For examples, the size of the subzone 1 for the rectangular teeth is a little larger than that for the corresponding trapezoidal teeth, which makes sizes of the subzones 2 and 3 for the rectangular teeth comparatively smaller. Therefore, in the case of the rectangular teeth, the material flows rapidly in these subzones and hence, the rates of internal deformation energy dissipation increase, and thus yield increase in the relative pressure. It may however, be seen from these figures that the relative pressures for the first stage for all these cases are in general, in the range of 1.0～3.4 except, for the tooth corner filling stage i.e. the second stage. During the tooth corner filling stage, the relative pressures in each of the cases for both the rectangular and trapezoidal teeth increase very rapidly.

Forging loads corresponding to the relative pressures Fig. 11(a) for the straight teeth and Fig. 11(b) for the tapered teeth for N_T=4 and 8, for the initial solid billet, during incremental forging of crown gear forms are shown in Figs. 12(a) and 12(b), respectively. It may be seen from these figures that in general the forging loads increase with increasing friction coefficient m and also the forging load in each case during the tooth corner filling stage increases very rapidly, as would be expected. Such a simulation result in each case is almost similar to that obtained from an upper bound solution [8] and the finite element analysis [19] for closed-die forging of the hexahedral and rectangular shapes.

Again, since at the tooth corner filling stage, as both the relative pressures and forging loads all increase rapidly, a highly pressing machine has to be in great demand to get to the final shape of the forged product. The excessive forging load that acts at that stage on the die-set, can cause increased die wear and decreased die-set life. Thus, there is a need to find a suitable alternative in order to get an excellent product. Perhaps, using a good preform shape of the initial billet can get the material flow during the forging to come simultaneously in contact with the tooth root of the punch without an abrupt initiation of the tooth corner filling stage and thus require somewhat less forging load

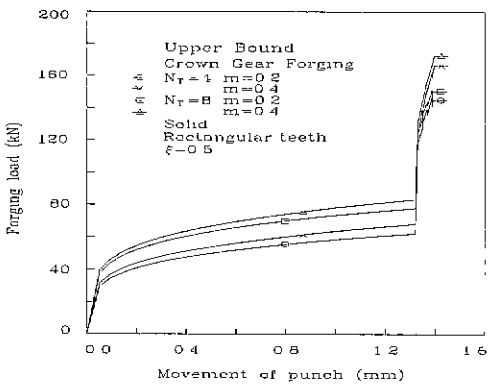

(a) Rectangular teeth

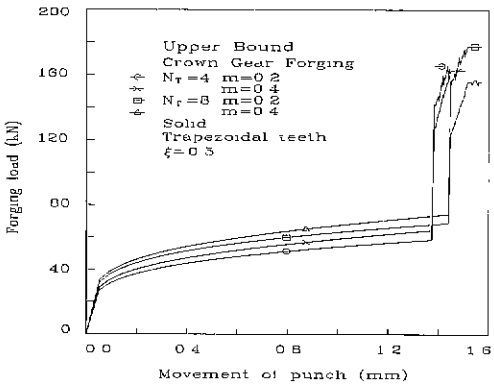

(b) Trapezoidal teeth

Fig. 12 Forging load respect to punch movement (solid billet, N_T=4 and 8, theoretical)

6.4 Comparison of experimental and theoretical results : die load-die movement curves

Typical Figs. 13(a) and 13(b) show the experimentally observed die load-die movement curves for Te-lead specimens which were earlier shown in Figs. 6(a) and 7(a). For comparison, the estimated values of the die loads at various die movement stages based on the upper bound analyses are also shown plotted therein.

Theoretical estimates of loads in crown gear forging for specimens of h_o/d_o=0.27, where h_o and d_o are height and diameter of the initial specimen respectively, were done on the assumption of friction factors, m=0.2 and 0.4. The number of gear in each tooth shape were kept at 4 and 8 while the whole tooth depth of each crown gear form was 3.8 mm. These are shown

compared with the experimentally observed values of die loads at increasing die movements. From these figures which show a comparison of the experimental and the theoretical die load-die movement curves for a specimen having eight teeth, it is observed that the theoretical results lie very close to those observed experimentally. It is also seen that the die load values estimated using UBET are higher than those obtained by experiments. This may be because the subdivision of the deforming zone was made simplifying the velocity discontinuities linearly and also the velocity field for tooth part, i.e., subzone 4 assumed to flow plastically in the axial direction

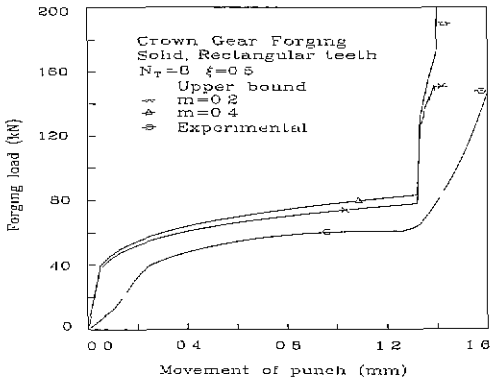

(a) Rectangular teeth

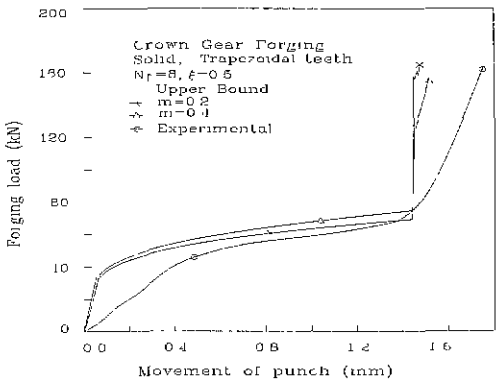

(b) Trapezoidal teeth

Fig. 13 Comparison of experimental and theoretical die load-die movement curves (N_T=8, solid specimen, ξ=0.5, h_o/d_o=0.27, d_o=38mm, h_t=3.8mm, r_f=8.9mm)

7. Conclusion

Near-net shape forging process for a crown gear with two of the simplified shapes of the crown gear form teeth, i.e., rectangular and trapezoidal teeth, was analysed for 4 and 8 teeth with initially solid and hollow circular cylindrical billets using the upper bound elemental simulation technique. A kinematically admissible velocity field corresponding to the forging process was presented using the velocity discontinuity boundaries assumed to be straight planes. Forging loads and deformation flow patterns obtained using the velocity field are presented and compared. According to the incremental upper bound simulation the results for the relative pressures for the near-net shape forging of the crown gear form with the 8 teeth, it was found that these values were in the range of 1.0 and 3.4 for the solid circular billets at the friction conditions of m=0.2 and 0.4 except, for the tooth corner filling stage, and these were in the range of 1.0 and 3.2 for the hollow billets under the same forging conditions. The forging load in each case increased rapidly after the initiation of the tooth corner filling stage.

References

1. Chen, C. C. and Kobayashi, S., "Rigid-plastic finite element analysis of plane-strain closed-die forging," Process Modelling, pp. 167-183, 1979.
2. Kobayashi, S, Oh, S. I., and Altan, T., "Metal Forming and the Finite-Element Method," New York, Oxford University Press, 1989.
3. Prager, W and Hodge, P. G., "Theory of Perfectly Plastic Solids." Chapman and Hall, London, 1951.
4. Kudo, H, "An upper-bound approach to plane-strain forging and extrusion-I,II," Int. J. Mech. Sci., Vol.1, pp.57-83, pp 229-252, 1960.
5. Kudo, H, "Some analytical and experimental studies of axisymmetric cold forging and extrusion-I,II," Int. J. Mech., Sci., Vol. 2, pp. 102-127, Vol. 3, pp. 91-117, 1960.
6. Kobayashi, S, "Upper-bound solution of axisymmetric forming problems-I,II." J. Eng. Ind. Trans., ASME, Vol. 86, pp. 112-126, pp. 326-332, 1964.
7. Avitzur, B, *Metal Forming: The Application of Limit Analysis*, Marcel Dekker Inc. New York, 1980.
8. Monaghan, J. M. and Torrance, A. A. "An Upper Bound Solution for Closed-Die Forging of Hexagonal and Square Workpieces," Int. J. Mech. Tool Des. Vol. 24, p. 225, 1984.

9. McDermott, R. P. and Bramley, A. N. "An elemental upper-bound technique for general use in forging analysis," 15th Int. Machine Tool Des. & Res. Conf., Birmingham, pp. 437-443, 1974.
10. Kiuchi, M. and Shigeta, S., "Application of upper-bound elemental technique to axisymmetric forging process," JSTP, Vol. 22, pp. 1208-1214, 1981.
11. Kiuchi, M. and Karato, A., "Application of upper-bound elemental technique to non-axisymmetric forging process," Advanced Technology of Plasticity, Vol. 2, pp. 967-872, 1984.
12. Lin, Y. T. and Wang, J. P., "A new upper-bound elemental technique approach to axisymmetric metal forming process," Int. J. Mach. Tools Manufact. Vol. 33, pp. 135-152, 1993.
13. Wang, J. P. and Lin, Y. T., "The load analysis of the plane-strain forging process using the upper-bound stream-function elemental technique," J. Mat. Proc. Tech., Vol. 47, pp. 345-359, 1995.
14. Juneja, B. L. and Grover, O. B., "Analysis of Forging Splines," J. Engng. Prod., Vol. 4, pp. 48-59, 1981.
15. Grover. O. P. and Juneja, B. L., "Analysis of closed-die forging of gear-like elements," Advanced Tech. of Plasticity, Vol.II, pp. 888-893, 1984.
16. Abdul, N. A. and Dean, T. A., "An analysis of the forging of spur gear forms," Int. J. Mach. Tool Des. Res., Vol. 26, pp. 113-123, 1986.
17. Kiuchi, M., Chung, H. K. and Yanagimoto, J., "Analysis of upsetting of hollow billets with square and gear-type dies," J. JSTP, Vol. 31, pp. 907-912, 1990.
18. Chitkara, N. R. and Kim, Y. J., "Upper bound analysis of near-net shaped forging of gear coupling forms," Int. J. Mech. Sci., Vol. 38, pp. 791-803, 1996.
19. Chen, C. C. and Kobayashi, S., "Rigid-Plastic Finite Element Analysis of Plane-Strain Closed-Die Forging," Process Modelling, pp.167-183, 1979.
20. Kim, Y. J. and Chitkara, N. R., "Determination of preform shape to improve dimensional accuracy of the forged crown gear form in a closed-die forging process," (To be published at Int. J. Mech. Sci.).